CoSMIC: Continual Self-supervised Learning for Multi-Domain Medical Imaging via Conditional Mutual Information Maximization

Supplementary Material

7. Conditional Mutual Information Maximization

7.1. Decouple Eq. 4

To maximize the conditional mutual information, we first decouple $\mathcal{I}(X_{\mathcal{D}_t}; Y_{\mathcal{D}_t}|Z_{\mathcal{D}_{t-1}})$ as the difference between (i) the information provided jointly by $X_{\mathcal{D}_t}$ and $Z_{\mathcal{D}_{t-1}}$ about $Y_{\mathcal{D}_t}$, and (ii) the information provided by $Z_{\mathcal{D}_{t-1}}$ alone about $Y_{\mathcal{D}_t}$. Mathematically, this can be expressed as:

$$\mathcal{I}(X_{\mathcal{D}_t}; Y_{\mathcal{D}_t}|Z_{\mathcal{D}_{t-1}}) = \mathcal{I}(Y_{\mathcal{D}_t}; X_{\mathcal{D}_t} Z_{\mathcal{D}_{t-1}}) - \mathcal{I}(Y_{\mathcal{D}_t}; Z_{\mathcal{D}_{t-1}}). \tag{14}$$

Here, $\mathcal{I}(Y_{\mathcal{D}_t}; Z_{\mathcal{D}_{t-1}})$ quantifies the mutual information between $Y_{\mathcal{D}_t}$ and the previously available knowledge $Z_{\mathcal{D}_{t-1}}$. Based on the definition and formulation of entropy, it can be expressed as:

$$\begin{aligned}
&\mathcal{I}(Y_{\mathcal{D}_t}; Z_{\mathcal{D}_{t-1}}) = H(Y_{\mathcal{D}_t}) - H(Y_{\mathcal{D}_t} \mid Z_{\mathcal{D}_{t-1}}) \\
&= \sum_{Y_{\mathcal{D}_t}} P(y) \log \frac{1}{P(y)} - \sum_{Y_{\mathcal{D}_t}} \sum_{Z_{\mathcal{D}_{t-1}}} P(yz) \log \frac{1}{P(y|z)} \\
&= \sum_{Y_{\mathcal{D}_t}} \sum_{Z_{\mathcal{D}_{t-1}}} P(yz) \log \frac{1}{P(y)} - \sum_{Y_{\mathcal{D}_t}} \sum_{Z_{\mathcal{D}_{t-1}}} P(yz) \log \frac{1}{P(y|z)} \\
&= \sum_{Y_{\mathcal{D}_t}} \sum_{Z_{\mathcal{D}_{t-1}}} P(yz) \log \frac{P(y|z)}{P(y)}.
\end{aligned} \tag{15}$$

Similarly, the mutual information between $Y_{\mathcal{D}_t}$ and the joint variable $(X_{\mathcal{D}_t}, Z_{\mathcal{D}_{t-1}})$ can be expressed in terms of entropy as:

$$\begin{aligned}
&\mathcal{I}(Y_{\mathcal{D}_t}; X_{\mathcal{D}_t} Z_{\mathcal{D}_{t-1}}) = H(Y_{\mathcal{D}_t}) - H(Y_{\mathcal{D}_t} \mid X_{\mathcal{D}_t} Z_{\mathcal{D}_{t-1}}) \\
&= \sum_{Y_{\mathcal{D}_t}} P(y) \log \frac{1}{P(y)} - \sum_{X_{\mathcal{D}_t}} \sum_{Y_{\mathcal{D}_t}} \sum_{Z_{\mathcal{D}_{t-1}}} P(xyz) \log \frac{1}{P(y|xz)} \\
&= \sum_{X_{\mathcal{D}_t}} \sum_{Y_{\mathcal{D}_t}} \sum_{Z_{\mathcal{D}_{t-1}}} P(xyz) \log \frac{1}{P(y)} \\
&- \sum_{X_{\mathcal{D}_t}} \sum_{Y_{\mathcal{D}_t}} \sum_{Z_{\mathcal{D}_{t-1}}} P(xyz) \log \frac{1}{P(y|xz)} \\
&= \sum_{X_{\mathcal{D}_t}} \sum_{Y_{\mathcal{D}_t}} \sum_{Z_{\mathcal{D}_{t-1}}} P(xyz) \log \frac{P(y|xz)}{P(y)}.
\end{aligned} \tag{16}$$

By substituting the expression of Eq. 15 and Eq. 16 into the Eq. 14 for conditional mutual information:

$$\begin{aligned}
&\mathcal{I}(Y_{\mathcal{D}_t}; X_{\mathcal{D}_t} \mid Z_{\mathcal{D}_{t-1}}) \\
&= \sum_{X_{\mathcal{D}_t}} \sum_{Y_{\mathcal{D}_t}} \sum_{Z_{\mathcal{D}_{t-1}}} P(xyz) \log \frac{P(y|xz)}{P(y)} \\
&- \sum_{Y_{\mathcal{D}_t}} \sum_{Z_{\mathcal{D}_{t-1}}} P(yz) \log \frac{P(y|z)}{P(y)} \\
&= \sum_{X_{\mathcal{D}_t}} \sum_{Y_{\mathcal{D}_t}} \sum_{Z_{\mathcal{D}_{t-1}}} P(xyz) \log \frac{P(y|xz)}{P(y)} \\
&- \sum_{X_{\mathcal{D}_t}} \sum_{Y_{\mathcal{D}_t}} \sum_{Z_{\mathcal{D}_{t-1}}} P(xyz) \log \frac{P(y|z)}{P(y)} \\
&= \sum_{X_{\mathcal{D}_t}} \sum_{Y_{\mathcal{D}_t}} \sum_{Z_{\mathcal{D}_{t-1}}} P(xyz) \log \frac{P(y|xz)}{P(y|z)}
\end{aligned} \tag{17}$$

Thus, the conclusion expressed in Eq. 4 can be obtained.

7.2. Optimization of Eq. 4

Similar to approximate $\mathcal{I}(X;Y)$ using a lower bound for optimization purposes, we also aim to find a tractable lower bound for the conditional mutual information: $\mathcal{I}(X_{\mathcal{D}_t}; Y_{\mathcal{D}_t}|Z_{\mathcal{D}_{t-1}})$. Since $\log x$ is a strictly convex function, applying Jensen's inequality to Eq. 4 gives:

$$\mathcal{I}(X_{\mathcal{D}_t}; Y_{\mathcal{D}_t}|Z_{\mathcal{D}_{t-1}}) \geq \log \sum_{X_{\mathcal{D}_t}} \sum_{Y_{\mathcal{D}_t}} \sum_{Z_{\mathcal{D}_{t-1}}} P(xyz) \frac{P(y|xz)}{P(y|z)} \tag{18}$$

Therefore, we only need to optimize this lower bound of $\mathcal{I}(X_{\mathcal{D}_t}; Y_{\mathcal{D}_t}|Z_{\mathcal{D}_{t-1}})$. However, as illustrated in Fig. 3(b), we encounter two key scenarios:

(i) When y and the joint representation $[xz]$ are incompatible, $P(y|xz) = P(y)$ and $P(xyz) = P(y)P(xz)$.

Therefore, Eq.5 is collapsed as:

$$
\begin{aligned}
&\log \sum_{X_{\mathcal{D}_t}} \sum_{Y_{\mathcal{D}_t}} \sum_{Z_{\mathcal{D}_{t-1}}} P(xyz) \frac{P(y|xz)}{P(y|z)} \\
&= \log \sum_{X_{\mathcal{D}_t}} \sum_{Y_{\mathcal{D}_t}} \sum_{Z_{\mathcal{D}_{t-1}}} P(xyz) \frac{P(y)}{\sum_{X_{\mathcal{D}_t}} P(xy|z)} \\
&= \log \sum_{X_{\mathcal{D}_t}} \sum_{Y_{\mathcal{D}_t}} \sum_{Z_{\mathcal{D}_{t-1}}} P(xyz) \frac{P(y)}{\sum_{X_{\mathcal{D}_t}} P(y|xz)P(x|z)} \\
&= \log \sum_{X_{\mathcal{D}_t}} \sum_{Y_{\mathcal{D}_t}} \sum_{Z_{\mathcal{D}_{t-1}}} P(xyz) \frac{P(y)}{P(y)\sum_{X_{\mathcal{D}_t}} P(x|z)} \\
&= \log \sum_{X_{\mathcal{D}_t}} \sum_{Y_{\mathcal{D}_t}} \sum_{Z_{\mathcal{D}_{t-1}}} P(xyz) \\
&= \log \sum_{X_{\mathcal{D}_t}} \sum_{Y_{\mathcal{D}_t}} \sum_{Z_{\mathcal{D}_{t-1}}} P(y)P(xz) \\
&= \log \sum_{Y_{\mathcal{D}_t}} P(y) \sum_{x_{\mathcal{D}_t}} \sum_{Z_{\mathcal{D}_{t-1}}} P(xz) \\
&= \log \sum_{Y_{\mathcal{D}_t}} P(y) \\
&= \log 1 = 0
\end{aligned}
\tag{19}
$$

(ii) when y and x are incompatible, $P(y|xz) = P(y|z)$. Therefore, Eq.5 is collapsed as:

$$
\begin{aligned}
&\log \sum_{X_{\mathcal{D}_t}} \sum_{Y_{\mathcal{D}_t}} \sum_{Z_{\mathcal{D}_{t-1}}} P(xyz) \frac{P(y|xz)}{P(y|z)} \\
&= \log \sum_{X_{\mathcal{D}_t}} \sum_{Y_{\mathcal{D}_t}} \sum_{Z_{\mathcal{D}_{t-1}}} P(xzy) \frac{P(y|z)}{P(y|z)} \\
&= \log \sum_{X_{\mathcal{D}_t}} \sum_{Y_{\mathcal{D}_t}} \sum_{Z_{\mathcal{D}_{t-1}}} P(z)P(x|z)P(y|xz) \\
&= \log \sum_{X_{\mathcal{D}_t}} P(x|z) \sum_{Y_{\mathcal{D}_t}} P(y|xz) \sum_{Z_{\mathcal{D}_{t-1}}} P(z) \\
&= \log \sum_{X_{\mathcal{D}_t}} P(x|z) \sum_{Y_{\mathcal{D}_t}} P(y|xz) = \log \sum_{X_{\mathcal{D}_t}} P(x|z) \\
&= \log 1 = 0
\end{aligned}
\tag{20}
$$

These suggests that the optimization of Eq. 5 is effectively proportional to maximizing the similarity of both $\text{sim}([XZ]_{\mathcal{D}_t}, Y_{\mathcal{D}_t})$ and $\text{sim}(X_{\mathcal{D}_t}, Y_{\mathcal{D}_t})$ for all image views.

8. Fine-tuning Setting

In most of our downstream tasks, we maintain a consistent and simplified experimental configuration that aligns with the default settings of [70, 71]. We deliberately avoid dataset-specific or model-specific hyperparameter tuning, including for our proposed CoSMIC, ensuring both the fairness of experimental comparisons and the reproducibility of our proposed model.

8.1. Multi-class and Binary-class Classification

For all datasets in this task—including APTOS, Glaucoma, IDRiD, PAPILA, Retina, ZhangCXR, RSNA, ISIC2016, ISIC2017, ISIC2018, and NCH—we strictly follow the fine-tuning configurations outlined in RETFound [71].

The training process employs the AdamW optimizer with a batch size of 128 per GPU, running for 50 epochs on a single NVIDIA A6000 GPU. The base learning rate is initialized at 5e-3 and dynamically adjusted via layer-wise decay, with a warmup phase over the first 10 epochs and a lower bound of 1e-6.

All input images are resized to 256 256 using cubic interpolation, followed by random cropping, where crop sizes range from 20% to 100% of the original image dimensions, producing patches of 224×224. To enhance training robustness, Mixup and Cutmix are applied with alpha values set to 0 and a probability of 1.0.

8.2. Multi-label Classification

Multi-label classification predicts multiple disease labels from a single image, unlike traditional single-label classification, where each patient is diagnosed with only one disease. This approach better reflects real-world clinical scenarios, where patients may present with multiple conditions simultaneously. To evaluate our model's effectiveness in multi-label classification, we use two open-source medical datasets.

Specifically, we evaluate multi-label classification performance on: **(i) NIH**: A dataset comprising 112,120 frontal-view chest X-rays (CXRs) from 30,805 unique patients, annotated with 14 disease labels: Atelectasis (Atel.), Cardiomegaly (Card.), Consolidation (Cons.), Edema (Edem.), Effusion (Effu.), Emphysema (Emph.), Fibrosis (Fibr.), Hernia (Hern.), Infiltration (Infi.), Mass (Mass.), Nodule (Nodu.), Pleural Thickening (P.E.), Pneumonia (Pneu.), and Pneumothorax (PneuX.). **(ii) CXP**: A dataset containing 224,316 CXRs from 65,240 patients. Following the original study, we conduct multi-label classification for Atelectasis (Atel.), Cardiomegaly (Card.), Edema (Edem.), Consolidation (Cons.), and Pleural Effusion (P.E.).

During training, we use the Stochastic Gradient Descent (SGD) optimizer with a momentum of 0.9. A cosine learning rate scheduler with linear warmup (50 warmup steps) dynamically adjusts the learning rate throughout the training process. The model is trained for: (i) 200,000 steps under 100% labeling rate, with a learning rate of 3e-3; (ii) 3,000 steps under 10% labeling rate, with a learning rate of 3e-3; and (iii) 2,000 steps under 1% labeling rate, with

a learning rate of 8.5e-3. All training is performed with a batch size of 96 on a single NVIDIA A6000 GPU. The loss function used is Binary Cross-Entropy with Logits (BCEWithLogitsLoss). Validation is conducted every 10 epochs, and the model with the highest validation AUC is saved for evaluation. Input images are resized to 224×224, and data augmentation techniques such as random cropping and horizontal flipping are applied within the data loader to enhance generalization.

8.3. Segmentation

For segmentation fine-tuning, we use an input resolution of 512×512. The optimization process employs the AdamW optimizer with a learning rate of 2e-5, betas set to (0.9, 0.999), and a weight decay of 0.05. To further enhance optimization, a layer-wise learning rate decay (rate = 0.65) is applied across 12 transformer layers. The learning rate follows a polynomial decay schedule with a linear warmup phase over 1,500 iterations (warmup ratio = 1e-6) and a minimum learning rate of 0.0, adjusted on a per-iteration basis. Training is conducted using mixed precision (FP16) with dynamic loss scaling across 4 NVIDIA A6000 GPUs. Checkpoints are saved every 10,000 iterations, and evaluations are performed every 500 iterations, with the best model selected based on the highest Dice score achieved during validation.

9. Visualizations

9.1. Qualitative Analysis of Segmentation Performance

For a qualitative comparison, we visualized the segmentation results on SIIM-ARC, as shown in Fig. 7. The results demonstrate that the proposed CoSMIC effectively captures pathological regions, exhibiting significant overlap between the predicted and ground truth regions. The contours and shapes of the segmented areas are well-aligned, indicating that CoSMIC successfully learns abnormality patterns. Notably, CoSMIC maintains strong segmentation performance even in challenging cases, such as irregularly shaped abnormalities (Fig. 7 (a) and (d)) or low-contrast regions (Fig. 7 (b) and (e)), highlighting its robustness in challenging scenarios.

9.2. t-SNE Visualization of Multi-Domain Representations

We visualized the learned representations using t-SNE, randomly selecting 10K samples from each pre-trained domain for analysis. The results, presented in Fig. 8, provide key insights into the effectiveness of different training paradigms for multi-domain medical representation learning. Specifically, we compare representations obtained from models: supervised on ImageNet (Fig. 8 (a), ViT), supervised on multi-domain medical images (Fig. 8 (b), RedImageNet), self-supervised on multi-domain medical images (Fig. 8 (c), LVM-Med), jointly self-supervised on multi-domain medical images using our proposed $\mathcal{L}_{CosMIC}$ (Fig. 8 (d), Joint), state-of-the-art continual self-supervised learning (SSL) on multi-domain medical images (Fig. 8 (e), MedCoSS), and our proposed CoSMIC (Fig. 8 (f)). In this experiment, we incrementally pre-trained CosMIC in the $\mathcal{D}_5$ domain to align other models.

When training on data from multiple domains simultaneously, as seen in Fig. 8 (a), (b), (c), (d), the learned representations appear scattered, lacking clear classification boundaries. This dispersion suggests that joint pre-training struggles to effectively capture and differentiate domain-specific knowledge. In contrast, MedCoSS, which employs a sequential pre-training approach, produces more compact and well-separated clusters, indicating better preservation of modality-specific characteristics.

Notably, our proposed CoSMIC further enhances the separation and organization of domain-specific clusters, surpassing MedCoSS. This suggests that CoSMIC not only promotes greater intra-domain compactness but also improves inter-domain distinction, demonstrating its superior effectiveness in multi-domain medical image analysis.

10. Details of Statistical Analysis

(i) The detailed evaluation metric scores for multi-label classification, corresponding to Table 2 and Fig. 4, are provided in Table 4 (CXP dataset) and Table 5 (OCT2017 dataset).

(ii) The evaluation metric scores for the comparison with unified pre-training models on downstream multi-domain medical imaging tasks, corresponding to Fig. 5, are reported in Table 6.

(iii) The evaluation metric scores for the comparison with continual self-supervised learning (SSL) models on downstream multi-domain medical imaging tasks, corresponding to Fig. 6, are provided in Table 7.

The training codes and pre-trained weights are available at https://github.com/LYH-hh/CoSMIC_ICCV.

11. Limitation

In the current CoSMIC framework, learning new knowledge primarily relies on an additional decoder for image reconstruction. While this strategy is effective in enhancing image representations, it introduces additional computational overhead. Therefore, future work will focus on exploring a more efficient approach, particularly from the perspective of mutual information, to learn new knowledge during each incremental pretraining phase. We aim to directly optimize shared features of multi-domain representations through a refined mutual information maximization

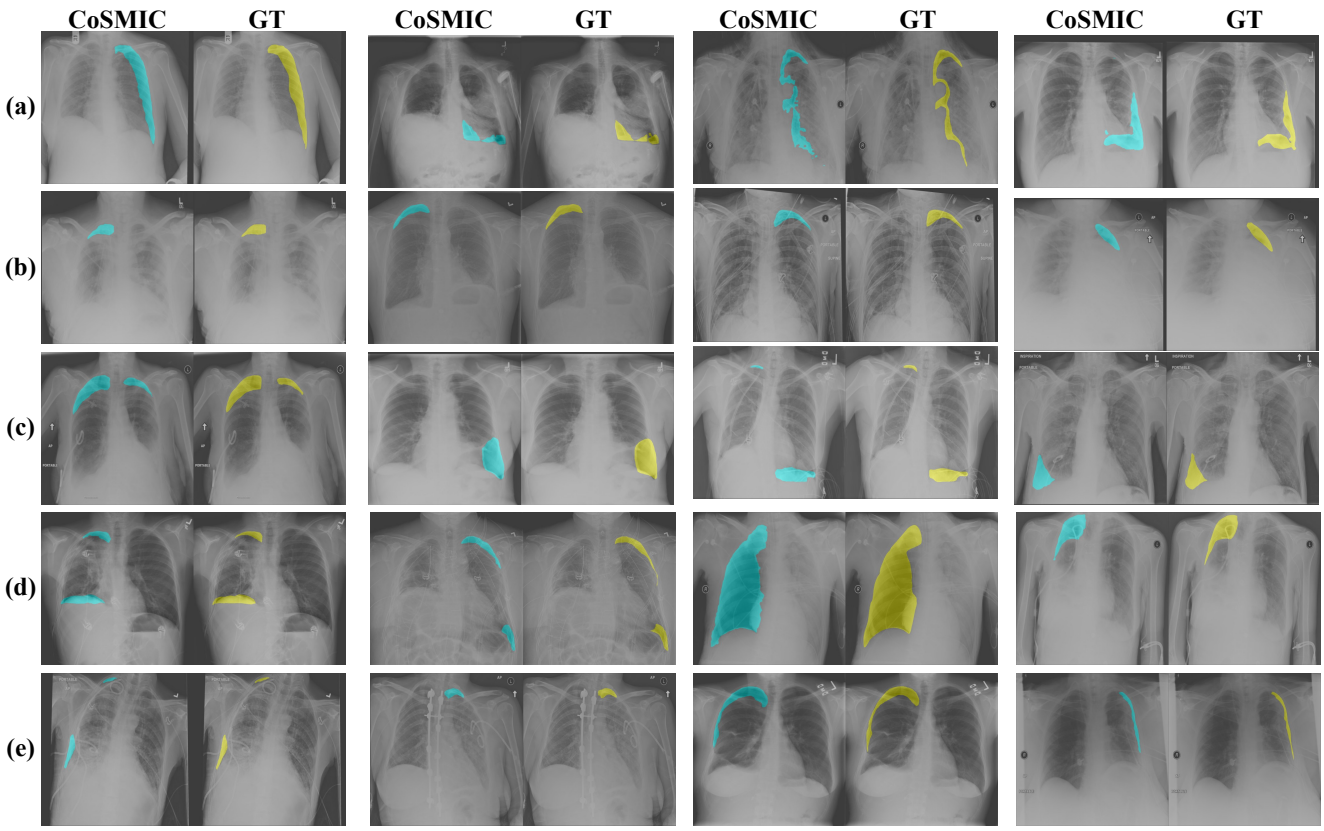

Figure 7. **Visualization of segmentation results on SIIM**. The results predicted by CoSMIC are colored blue and the Ground Truth (GT) are colored yellow.

mechanism, avoiding the reliance on the reconstruction process with a decoder, thereby reducing computational cost and improving training efficiency.

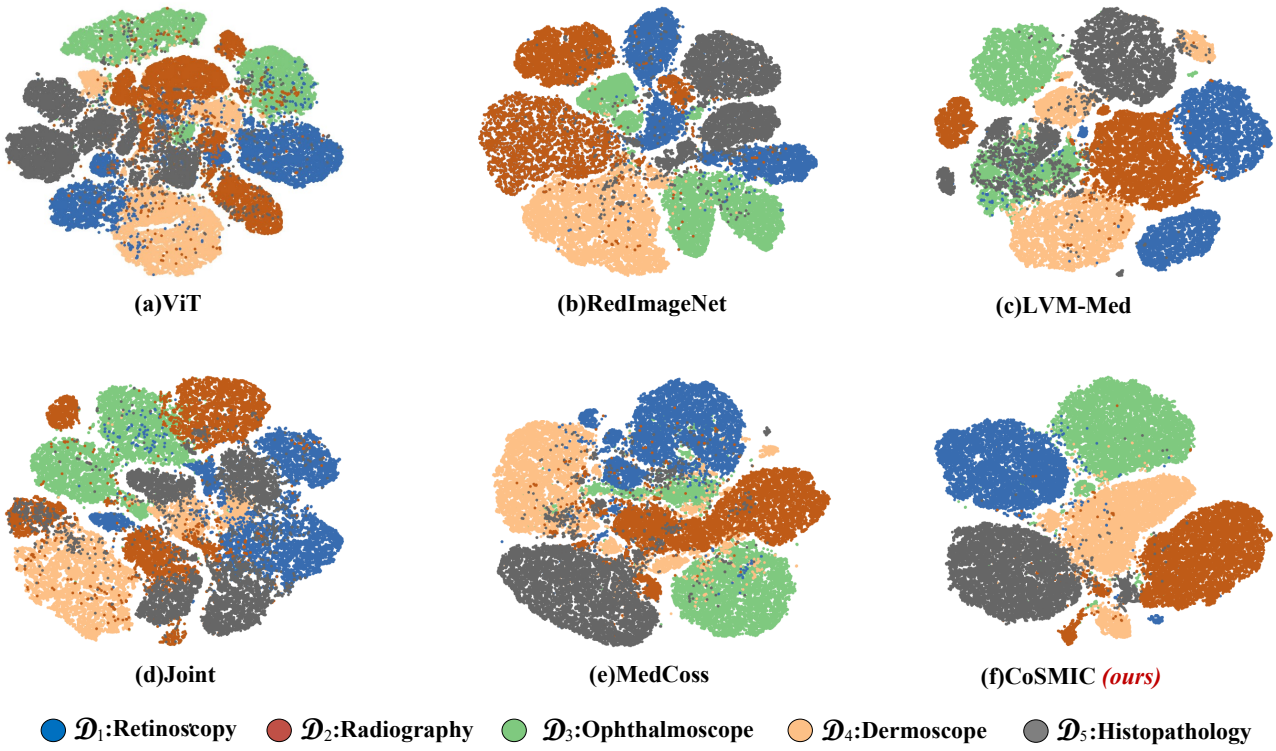

Figure 8. **t-SNE visualizations of visual representations** extracted from ViT, joint-pre-training medical foundation models: RedImageNet(supervised) and LVM-Med (self-supervised), joint-pre-training using our $\mathcal{L}_{CoSMIC}$, continual SSL medical medical foundation model MedCoss, and our CoSMIC on four medical domain data.

Ratio	Model	Atel	Card	Edema	Cons	P.E.	Mean
1%	DINO	72.60±0.06	78.20±0.09	87.40±0.21	81.70±0.06	83.20±0.11	80.62±0.11
	MAE	77.90±0.07	80.60±0.11	89.70±0.07	74.80±0.01	82.90±0.13	81.18±0.28
	C2L	74.30±0.03	79.40±0.12	84.50±0.06	85.90±0.18	80.20±0.01	80.86±0.03
	MG	71.40±0.04	71.50±0.06	86.70±0.08	84.60±0.05	81.80±0.19	79.20±0.02
	POPAR	69.20±0.07	79.80±0.06	87.20±0.02	84.30±0.00	82.40±0.09	80.58±0.01
	PEAC	72.30±0.07	75.70±0.01	88.40±0.16	82.40±0.20	83.40±0.18	80.44±0.05
	DiRA	73.50±0.05	76.80±0.21	84.20±0.09	87.80±0.01	85.20±0.03	81.50±0.09
	cxrMAE	74.90±0.08	78.30±0.08	87.40±0.12	89.60±0.08	82.30±0.15	82.50±0.10
	Adamv1	75.80±0.05	75.40±0.15	87.70±0.17	86.90±0.04	82.90±0.01	81.74±0.14
	Adamv2	77.50±0.05	74.80±0.02	88.10±0.30	87.30±0.05	84.40±0.10	82.42±0.08
	PCRLv1	73.80±0.20	75.90±0.04	81.70±0.13	84.20±0.16	88.90±0.15	80.90±0.09
	PCRLv2	74.20±0.22	76.40±0.06	85.90±0.11	85.60±0.18	88.30±0.20	82.08±0.15
	$\mathcal{D}_0$	76.40±0.02	79.80±0.03	86.90±0.02	77.70±0.08	84.20±0.07	81.00±0.04
	$\mathcal{D}_0 \rightarrow \mathcal{D}_1$	76.50±0.14	79.40±0.12	86.70±0.11	77.60±0.02	83.80±0.02	79.98±0.05
	$\mathcal{D}_0 \rightarrow \mathcal{D}_1 \rightarrow \mathcal{D}_2$	75.60±0.19	79.90±0.17	87.50±0.09	86.40±0.10	89.60±0.04	83.80±0.04
	$\mathcal{D}_0 \rightarrow \mathcal{D}_1 \rightarrow \mathcal{D}_2 \rightarrow \mathcal{D}_3$	75.20±0.22	79.50±0.18	87.60±0.10	85.90±0.01	89.40±0.09	83.52±0.05
	$\mathcal{D}_0 \rightarrow \mathcal{D}_1 \rightarrow \mathcal{D}_2 \rightarrow \mathcal{D}_3 \rightarrow \mathcal{D}_4$	74.90±0.19	79.50±0.03	87.50±0.03	85.60±0.11	89.10±0.16	83.32±0.12
10%	DINO	76.40±0.13	80.30±0.13	89.80±0.22	79.60±0.24	86.20±0.08	82.46±0.03
	MAE	78.80±0.06	82.40±0.08	90.70±0.16	78.90±0.17	86.40±0.09	83.44±0.14
	C2L	76.80±0.22	79.90±0.06	85.30±0.09	87.10±0.09	83.40±0.21	82.50±0.08
	MG	74.40±0.06	76.30±0.04	88.40±0.10	85.70±0.02	85.90±0.19	82.14±0.03
	POPAR	73.70±0.12	80.70±0.26	89.50±0.08	86.90±0.01	84.10±0.04	82.98±0.03
	PEAC	75.60±0.04	77.40±0.11	90.40±0.34	85.70±0.07	87.80±0.17	83.38±0.02
	DiRA	77.30±0.16	79.40±0.10	85.70±0.16	89.10±0.04	87.30±0.07	83.76±0.02
	cxrMAE	77.50±0.10	81.20±0.14	89.20±0.10	90.40±0.03	88.70±0.02	85.40±0.29
	Adamv1	76.90±0.14	78.10±0.17	89.50±0.03	89.60±0.05	86.40±0.33	84.10±0.13
	Adamv2	78.20±0.08	76.80±0.02	90.70±0.06	88.80±0.23	89.90±0.03	84.88±0.02
	PCRLv1	75.70±0.20	77.40±0.18	86.40±0.12	87.30±0.01	90.70±0.03	83.50±0.10
	PCRLv2	76.10±0.16	78.30±0.03	87.30±0.10	87.10±0.15	91.80±0.04	84.12±0.17
	$\mathcal{D}_0$	77.80±0.14	81.90±0.15	88.60±0.10	80.70±0.10	86.40±0.08	82.08±0.02
	$\mathcal{D}_0 \rightarrow \mathcal{D}_1$	77.60±0.14	81.70±0.09	88.60±0.18	80.40±0.07	86.30±0.03	81.92±0.29
	$\mathcal{D}_0 \rightarrow \mathcal{D}_1 \rightarrow \mathcal{D}_2$	78.30±0.11	82.50±0.03	90.30±0.12	89.80±0.13	91.60±0.15	86.50±0.21
	$\mathcal{D}_0 \rightarrow \mathcal{D}_1 \rightarrow \mathcal{D}_2 \rightarrow \mathcal{D}_3$	78.00±0.03	82.50±0.08	90.50±0.12	89.70±0.02	91.60±0.18	86.46±0.03
	$\mathcal{D}_0 \rightarrow \mathcal{D}_1 \rightarrow \mathcal{D}_2 \rightarrow \mathcal{D}_3 \rightarrow \mathcal{D}_4$	77.80±0.26	82.40±0.12	90.30±0.23	89.70±0.15	91.50±0.06	86.34±0.05
100%	DINO	82.20±0.18	85.40±0.02	91.60±0.09	84.90±0.10	89.80±0.16	86.78±0.18
	MAE	81.40±0.04	85.60±0.02	92.70±0.08	83.20±0.10	90.40±0.25	86.66±0.03
	C2L	81.10±0.19	81.40±0.09	92.90±0.14	93.00±0.06	92.60±0.11	88.20±0.10
	MG	79.80±0.05	80.00±0.09	91.50±0.09	91.30±0.06	90.90±0.06	86.70±0.08
	POPAR	80.70±0.31	83.10±0.01	91.60±0.25	90.90±0.07	92.30±0.19	87.72±0.12
	PEAC	81.50±0.03	82.70±0.04	92.80±0.21	89.60±0.25	93.20±0.13	87.96±0.05
	DiRA	80.50±0.07	83.20±0.12	90.30±0.15	92.60±0.14	90.70±0.04	87.46±0.02
	cxrMAE	82.70±0.26	83.50±0.27	92.50±0.18	93.80±0.01	94.10±0.08	89.32±0.02
	Adamv1	81.60±0.12	80.40±0.18	91.60±0.11	92.90±0.19	92.40±0.02	87.78±0.05
	Adamv2	82.20±0.24	81.60±0.02	92.10±0.19	91.50±0.13	93.30±0.03	88.14±0.06
	PCRLv1	80.40±0.14	82.30±0.07	91.70±0.03	90.60±0.09	93.50±0.15	87.70±0.07
	PCRLv2	81.60±0.22	83.20±0.13	92.30±0.05	90.70±0.08	93.40±0.08	88.24±0.22
	$\mathcal{D}_0$	81.50±0.14	84.20±0.13	92.20±0.05	84.30±0.06	88.80±0.20	86.20±0.04
	$\mathcal{D}_0 \rightarrow \mathcal{D}_1$	81.20±0.04	84.30±0.27	92.10±0.24	84.10±0.35	88.90±0.25	86.12±0.06
	$\mathcal{D}_0 \rightarrow \mathcal{D}_1 \rightarrow \mathcal{D}_2$	82.70±0.02	85.40±0.06	93.50±0.06	92.60±0.05	94.70±0.03	89.78±0.03
	$\mathcal{D}_0 \rightarrow \mathcal{D}_1 \rightarrow \mathcal{D}_2 \rightarrow \mathcal{D}_3$	82.50±0.12	85.40±0.09	93.40±0.18	92.40±0.19	94.50±0.17	89.64±0.02
	$\mathcal{D}_0 \rightarrow \mathcal{D}_1 \rightarrow \mathcal{D}_2 \rightarrow \mathcal{D}_3 \rightarrow \mathcal{D}_4$	82.40±0.06	85.20±0.12	93.40±0.10	92.40±0.15	94.40±0.14	89.56±0.15

Table 4. **Comparisons of multi-label classification on the CXP dataset.** The AUC score ↑ (%) of each disease is reported.

Ratio	Model	Atel	Card	Effu	Infi	Mass	Nodu	Pneu	PneuX	Cons	Edem	Emph	Fibr	P.T.	Hern	Mean
1%	DINO	56.92±0.10	49.94±0.33	61.75±0.11	49.94±0.14	58.78±0.15	51.89±0.01	55.43±0.06	63.61±0.21	65.01±0.09	70.12±0.15	62.22±0.39	55.52±0.29	61.66±0.16	53.38±0.14	58.30±0.11
	MAE	57.10±0.04	49.20±0.20	62.96±0.02	47.80±0.11	59.61±0.19	50.50±0.34	53.57±0.13	67.24±0.17	63.61±0.04	71.05±0.14	65.38±0.16	54.78±0.19	59.89±0.13	54.78±0.18	58.39±0.10
	C2L	56.64±0.04	50.31±0.14	63.05±0.06	48.64±0.03	58.03±0.01	52.27±0.06	57.01±0.20	68.73±0.12	61.10±0.06	75.61±0.09	67.15±0.18	57.01±0.01	62.96±0.22	57.19±0.06	59.69±0.04
	MG	55.52±0.12	49.76±0.04	63.43±0.06	49.66±0.25	60.26±0.03	55.52±0.14	58.03±0.14	68.63±0.04	62.59±0.01	72.45±0.20	64.64±0.06	55.52±0.04	61.75±0.26	50.96±0.05	59.19±0.17
	POPAR	58.31±0.27	51.80±0.14	65.01±0.05	49.01±0.22	63.05±0.10	56.64±0.02	59.80±0.21	69.56±0.14	67.70±0.04	74.68±0.09	69.38±0.10	57.47±0.02	59.89±0.08	53.29±0.14	61.11±0.02
	PEAC	59.43±0.03	49.57±0.05	63.61±0.08	47.80±0.11	62.03±0.10	55.24±0.13	61.57±0.20	66.96±0.05	70.96±0.05	77.10±0.05	69.10±0.27	57.10±0.15	58.40±0.01	54.59±0.14	60.96±0.01
	DiRA	60.82±0.14	52.45±0.07	65.01±0.12	50.03±0.04	62.77±0.23	57.10±0.08	66.77±0.25	71.05±0.12	67.52±0.14	74.21±0.03	68.26±0.04	58.31±0.08	67.33±0.32	54.96±0.12	62.62±0.04
	cxrMAE	66.68±0.19	62.40±0.02	72.82±0.06	55.43±0.02	67.61±0.06	57.20±0.14	64.73±0.05	72.82±0.12	65.47±0.15	76.63±0.06	67.70±0.25	62.22±0.03	65.19±0.12	58.40±0.07	65.38±0.02
	Adamv1	64.45±0.04	59.24±0.09	68.73±0.17	52.73±0.20	66.31±0.07	55.24±0.19	62.03±0.11	71.14±0.15	65.84±0.31	77.56±0.04	66.22±0.03	60.17±0.17	62.22±0.05	59.05±0.03	63.64±0.03
	Adamv2	64.08±0.09	62.22±0.14	71.98±0.05	53.85±0.23	64.26±0.12	58.31±0.12	63.15±0.28	73.10±0.04	66.40±0.18	78.12±0.04	67.52±0.04	60.82±0.09	61.10±0.25	59.89±0.04	64.63±0.12
	PCRLv1	64.36±0.07	59.89±0.23	71.33±0.17	55.15±0.30	66.31±0.20	56.54±0.21	60.82±0.05	71.98±0.22	67.24±0.07	74.68±0.01	69.10±0.03	59.24±0.15	64.82±0.08	57.10±0.32	64.18±0.03
	PCRLv2	63.52±0.13	61.38±0.04	73.28±0.02	56.08±0.19	65.75±0.17	57.57±0.25	63.24±0.06	73.38±0.08	67.89±0.11	75.70±0.08	68.73±0.06	60.26±0.10	65.56±0.15	57.94±0.21	65.02±0.10
	$\mathcal{D}_0$	56.54±0.15	48.73±0.09	63.05±0.02	47.99±0.05	60.17±0.12	50.50±0.02	55.52±0.22	64.36±0.14	62.68±0.12	69.56±0.04	64.91±0.04	54.31±0.22	59.24±0.07	53.10±0.09	57.91±0.22
	$\mathcal{D}_0 \rightarrow \mathcal{D}_1$	55.99±0.19	49.48±0.08	62.68±0.03	48.73±0.06	60.54±0.16	49.85±0.10	56.17±0.16	64.36±0.13	62.68±0.09	69.56±0.26	64.91±0.15	54.31±0.10	59.24±0.30	53.10±0.07	57.97±0.19
	$\mathcal{D}_0 \rightarrow \mathcal{D}_1 \rightarrow \mathcal{D}_2$	69.70±0.08	68.80±0.18	76.70±0.05	61.20±0.16	69.80±0.13	62.90±0.22	67.20±0.07	77.40±0.16	72.60±0.04	77.80±0.16	72.40±0.31	66.30±0.05	70.70±0.03	63.80±0.04	69.81±0.09
	$\mathcal{D}_0 \rightarrow \mathcal{D}_1 \rightarrow \mathcal{D}_2 \rightarrow \mathcal{D}_3$	66.30±0.06	70.80±0.10	73.70±0.10	60.80±0.20	66.20±0.03	64.30±0.03	66.50±0.05	77.90±0.22	73.20±0.11	76.40±0.23	71.90±0.10	67.80±0.22	70.20±0.02	64.40±0.19	69.31±0.10
	$\mathcal{D}_0 \rightarrow \mathcal{D}_1 \rightarrow \mathcal{D}_2 \rightarrow \mathcal{D}_3 \rightarrow \mathcal{D}_4$	67.20±0.11	69.70±0.14	74.90±0.08	62.30±0.04	66.70±0.15	64.20±0.36	67.10±0.01	77.50±0.22	72.30±0.12	75.40±0.13	71.30±0.04	67.40±0.07	69.20±0.23	61.80±0.22	69.07±0.22
10%	DINO	68.90±0.05	62.30±0.15	76.50±0.07	59.70±0.13	72.90±0.04	66.70±0.29	67.40±0.16	76.80±0.06	71.30±0.16	80.40±0.17	74.80±0.32	64.70±0.12	69.80±0.19	62.90±0.09	69.65±0.04
	MAE	68.40±0.13	63.70±0.32	76.90±0.24	60.40±0.07	73.20±0.11	65.70±0.13	67.90±0.21	76.20±0.05	72.60±0.08	81.90±0.06	76.20±0.04	63.90±0.20	70.50±0.11	63.80±0.02	70.09±0.19
	C2L	72.50±0 .11	68.00±0.04	81.30±0.01	62.40±0.18	75.80±0.10	67.20±0.27	70.20±0.14	80.60±0.07	74.80±0.14	85.40±0.02	78.40±0.09	68.30±0.06	72.20±0.04	66.10±0.17	73.09±0.03
	MG	69.90±0.11	65.60±0.27	79.20±0.12	59.40±0.14	72.90±0.11	64.30±0.11	67.00±0.05	77.90±0.13	72.00±0.22	82.30±0.13	75.80±0.14	65.90±0.19	69.60±0.17	59.40±0.03	70.09±0.11
	POPAR	72.40±0.22	65.80±0.22	79.40±0.02	61.80±0.02	76.70±0.12	64.90±0.09	66.80±0.17	78.50±0.09	76.30±0.09	85.40±0.20	79.80±0.15	66.90±0.02	70.40±0.17	63.80±0.08	72.06±0.13
	PEAC	72.70±0.00	63.90±0.04	80.20±0.04	60.90±0.03	74.80±0.11	68.60±0.02	70.70±0.16	79.60±0.03	78.10±0.25	86.70±0.08	79.40±0.16	65.20±0.29	71.90±0.19	64.30±0.07	72.64±0.05
	DiRA	74.80±0.16	72.90±0.03	81.90±0.11	64.70±0.08	79.20±0.02	67.90±0.15	75.30±0.04	83.40±0.04	79.90±0.16	84.60±0.03	76.90±0.07	68.70±0.03	76.50±0.10	65.30±0.06	75.14±0.08
	cxrMAE	75.10±0.07	74.30±0.07	83.90±0.09	66.90±0.15	80.60±0.13	68.40±0.06	75.90±0.08	82.40±0.17	76.50±0.03	88.40±0.22	79.50±0.07	70.40±0.14	75.80±0.07	66.70±0.03	76.06±0.01
	Adamv1	73.60±0.03	70.20±0.11	80.80±0.13	64.30±0.06	77.40±0.13	67.50±0.26	72.10±0.07	83.40±0.14	76.40±0.11	87.10±0.29	78.40±0.10	69.70±0.05	73.50±0.02	67.20±0.02	74.40±0.01
	Adamv2	75.20±0.07	71.30±0.10	81.50±0.02	63.90±0.22	78.10±0.06	68.40±0.11	71.80±0.02	84.60±0.28	77.30±0.10	88.70±0.12	79.60±0.04	71.20±0.14	73.60±0.01	68.70±0.11	75.28±0.05
	PCRLv1	75.40±0.23	70.60±0.16	84.20±0.28	65.50±0.02	78.90±0.01	69.60±0.05	72.70±0.16	83.50±0.10	77.60±0.05	88.50±0.07	80.80±0.06	71.30±0.11	74.80±0.01	67.60±0.13	75.79±0.07
	PCRLv2	76.80±0.02	72.00±0.10	85.60±0.17	66.80±0.32	80.20±0.08	71.00±0.18	74.00±0.09	84.80±0.19	78.90±0.05	89.80±0.07	82.20±0.08	72.60±0.25	76.20±0.06	69.70±0.12	77.19±0.13
	$\mathcal{D}_0$	66.40±0.06	59.30±0.04	72.90±0.07	56.60±0.17	71.30±0.13	59.50±0.10	65.70±0.16	74.90±0.04	71.80±0.09	79.40±0.08	76.10±0.09	62.80±0.13	67.10±0.02	61.40±0.28	67.51±0.14
	$\mathcal{D}_0 \rightarrow \mathcal{D}_1$	65.20±0.17	55.80±0.06	72.30±0.02	54.90±0.21	72.80±0.02	58.90±0.08	66.40±0.13	72.30±0.05	70.60±0.10	76.90±0.20	77.80±0.16	61.20±0.03	67.90±0.11	60.70±0.25	66.69±0.10
	$\mathcal{D}_0 \rightarrow \mathcal{D}_1 \rightarrow \mathcal{D}_2$	78.40±0.06	85.20±0.09	85.20±0.16	68.10±0.16	83.20±0.08	71.60±0.15	78.50±0.17	83.60±0.12	78.50±0.20	87.70±0.19	87.10±0.17	78.10±0.15	77.80±0.07	87.20±0.25	80.73±0.09
	$\mathcal{D}_0 \rightarrow \mathcal{D}_1 \rightarrow \mathcal{D}_2 \rightarrow \mathcal{D}_3$	77.50±0.05	85.20±0.14	83.90±0.04	67.30±0.21	81.90±0.06	69.40±0.02	75.60±0.18	83.40±0.18	77.30±0.04	87.10±0.07	86.50±0.11	76.30±0.14	75.20±0.04	85.00±0.22	79.40±0.06
	$\mathcal{D}_0 \rightarrow \mathcal{D}_1 \rightarrow \mathcal{D}_2 \rightarrow \mathcal{D}_3 \rightarrow \mathcal{D}_4$	77.80±0.08	83.40±0.05	84.00±0.07	66.60±0.06	82.30±0.20	68.30±0.15	76.20±0.12	83.10±0.05	77.10±0.06	86.70±0.17	86.20±0.11	76.60±0.04	74.70±0.02	83.90±0.02	79.06±0.05
100%	DINO	79.70±0.27	73.60±0.09	87.40±0.09	70.70±0.09	84.80±0.31	78.00±0.08	79.90±0.04	87.60±0.06	81.90±0.28	92.00±0.13	86.40±0.31	76.00±0.01	80.50±0.08	75.10±0.20	80.97±0.01
	MAE	79.30±0.08	74.50±0.12	88.10±0.20	71.20±0.08	83.90±0.16	76.70±0.02	78.70±0.02	87.10±0.06	83.60±0.10	90.20±0.16	87.30±0.13	77.40±0.17	81.10±0.05	74.30±0.02	80.96±0.08
	C2L	78.20±0.01	87.00±0.27	85.30±0.02	68.30±0.06	84.80±0.04	73.70±0.13	74.80±0.06	85.50±0.06	79.60±0.13	90.10±0.38	86.30±0.10	80.00±0.21	78.60±0.05	88.10±0.35	81.45±0.08
	MG	77.80±0.07	86.30±0.07	84.70±0.16	67.30±0.19	83.60±0.08	73.00±0.10	74.10±0.11	84.90±0.10	78.80±0.04	89.50±0.09	85.70±0.18	79.60±0.13	78.20±0.02	87.00±0.07	80.75±0.13
	POPAR	78.20±0.20	87.90±0.23	88.40±0.14	69.80±0.06	85.60±0.11	74.30±0.05	76.90±0.10	86.70±0.20	78.80±0.07	89.30±0.11	87.50±0.08	79.90±0.38	80.30±0.21	87.90±0.02	82.25±0.03
	PEAC	77.90±0.11	88.00±0.16	87.90±0.13	68.40±0.02	84.90±0.11	74.90±0.11	77.80±0.10	87.40±0.20	80.90±0.05	90.80±0.15	87.00±0.06	78.60±0.09	79.70±0.25	89.60±0.07	82.41±0.01
	DiRA	79.50±0.20	88.20±0.13	86.40±0.09	70.50±0.11	85.70±0.23	75.80±0.21	74.30±0.25	88.50±0.10	79.40±0.33	89.90±0.08	88.90±0.06	82.30±0.22	79.40±0.42	90.20±0.01	82.79±0.05
	cxrMAE	80.50±0.05	89.40±0.07	87.20±0.15	69.90±0.03	87.30±0.04	77.50±0.25	75.80±0.37	87.60±0.04	80.40±0.30	91.20±0.24	86.90±0.19	83.30±0.07	79.10±0.04	91.50±0.12	84.40±0.02
	Adamv1	79.90±0.04	87.50±0.29	86.80±0.09	70.30±0.10	86.10±0.20	75.40±0.05	74.30±0.18	88.20±0.11	78.90±0.04	90.70±0.10	88.40±0.42	80.70±0.05	80.90±0.21	90.90±0.04	82.79±0.15
	Adamv2	80.20±0.27	88.40±0.25	87.90±0.09	71.20±0.14	85.80±0.21	76.30±0.13	74.90±0.03	88.70±0.22	79.80±0.19	91.40±0.15	87.30±0.05	80.80±0.04	81.10±0.01	91.40±0.15	83.23±0.24
	PCRLv1	79.80±0.03	88.50±0.06	87.10±0.42	69.70±0.05	86.10±0.12	75.60±0.09	76.10±0.01	87.00±0.12	81.20±0.10	91.60±0.16	87.70±0.10	81.70±0.05	80.40±0.02	90.20±0.02	83.05±0.05
	PCRLv2	80.70±0.05	89.30±0.03	87.90±0.12	70.50±0.17	87.00±0.10	76.40±0.17	77.00±0.13	87.90±0.19	82.00±0.11	92.50±0.16	88.60±0.33	82.60±0.18	81.30±0.14	91.60±0.02	83.95±0.09
	$\mathcal{D}_0$	79.10±0.06	72.50±0.08	86.70±0.04	68.70±0.06	83.50±0.18	72.70±0.28	79.00±0.18	86.60±0.22	85.00±0.36	91.20±0.14	87.70±0.06	75.30±0.10	80.10±0.02	73.80±0.07	80.14±0.03
	$\mathcal{D}_0 \rightarrow \mathcal{D}_1$	78.70±0.08	73.15±0.09	87.30±0.18	68.20±0.03	83.10±0.09	73.40±0.14	78.70±0.24	86.80±0.09	84.70±0.03	90.60±0.13	87.90±0.17	75.80±0.02	80.90±0.05	74.40±0.21	80.26±0.22
	$\mathcal{D}_0 \rightarrow \mathcal{D}_1 \rightarrow \mathcal{D}_2$	82.50±0.02	91.90±0.09	88.70±0.16	71.30±0.19	88.40±0.12	75.60±0.29	79.50±0.23	89.30±0.03	81.40±0.21	91.70±0.08	92.30±0.09	83.90±0.18	82.70±0.12	92.30±0.18	85.11±0.05
	$\mathcal{D}_0 \rightarrow \mathcal{D}_1 \rightarrow \mathcal{D}_2 \rightarrow \mathcal{D}_3$	82.20±0.07	91.20±0.05	88.20±0.11	71.00±0.04	87.90±0.18	75.60±0.14	79.10±0.19	89.30±0.14	81.10±0.04	91.60±0.20	92.30±0.06	83.90±0.05	82.20±0.11	92.00±0.19	84.83±0.11
	$\mathcal{D}_0 \rightarrow \mathcal{D}_1 \rightarrow \mathcal{D}_2 \rightarrow \mathcal{D}_3 \rightarrow \mathcal{D}_4$	82.10±0.09	91.00±0.06	88.20±0.08	70.90±0.13	87.60±0.18	75.30±0.16	78.70±0.13	89.20±0.22	80.90±0.14	91.40±0.19	92.20±0.15	83.80±0.07	82.00±0.13	91.90±0.08	84.66±0.19

Table 5. **Comparisons of multi-label classification on the NIH dataset.** The AUC score ↑ (%) of each disease is reported

Methods	APTOS AUC↑ (%)	Glaucoma AUC↑ (%)	IDRiD AUC↑ (%)	PAPILA AUC↑ (%)	Retina AUC↑ (%)	NIH AUC↑ (%)	CXP AUC↑ (%)	ZhangCXR AUC↑ (%)	RSNA AUC↑ (%)	SIIM-ARC Dice↑ (%)	OCTID AUC↑ (%)	ISIC2016 AUC↑ (%)	ISIC2017 AUC↑ (%)	ISIC2018 AUC↑ (%)	ISIC2018(seg) Dice↑ (%)
Scratch	89.52±0.05	89.26±0.02	75.07±0.11	64.64±0.04	69.86±0.03	73.57±0.15	83.56±0.06	89.27±0.11	83.69±0.11	68.24±0.24	93.28±0.12	86.75±0.07	84.77±0.02	74.54±0.13	81.17±0.01
Joint	92.13±0.08	91.16±0.01	79.87±0.02	76.46±0.03	85.39±0.05	81.49±0.07	86.97±0.18	96.12±0.01	87.57±0.25	78.35±0.07	97.67±0.09	93.02±0.04	93.76±0.16	91.54±0.15	87.09±0.36
ViT	92.30±0.05	90.64±0.01	80.17±0.11	76.70±0.06	73.17±0.09	80.14±0.03	86.20±0.04	96.15±0.09	92.00±0.14	72.82±0.53	95.59±0.13	91.55±0.05	95.20±0.11	90.35±0.08	86.48±0.04
DINO	92.71±0.18	90.15±0.07	80.29±0.07	74.52±0.13	76.43±0.26	80.97±0.01	86.78±0.16	96.78±0.04	92.32±0.18	70.92±0.76	94.37±0.16	90.22±0.33	92.45±0.14	92.19±0.33	87.05±0.05
MAE	92.22±0.04	91.86±0.04	78.40±0.08	72.65±0.04	72.61±0.07	80.96±0.07	86.66±0.02	95.88±0.15	91.84±0.14	73.58±1.14	95.17±0.06	91.56±0.26	93.71±0.30	91.47±0.05	86.41±0.05
CaSSLe	91.87±0.04	90.31±0.03	79.58±0.20	76.29±0.01	85.08±0.10	79.38±0.10	87.86±0.30	97.58±0.12	89.58±0.22	79.77±0.16	97.86±0.14	90.20±0.18	94.65±0.03	87.85±0.13	84.18±0.08
MedCoss	93.07±0.02	91.08±0.13	80.16±0.03	77.98±0.20	85.93±0.04	81.84±0.02	88.34±0.03	98.16±0.16	90.79±0.14	82.19±0.30	98.48±0.02	92.55±0.13	95.31±0.09	92.62±0.22	87.52±0.12
LVM-Med	92.67±0.10	92.26±0.09	80.31±0.13	78.84±0.02	85.27±0.02	83.39±0.07	87.65±0.25	97.81±0.03	90.36±0.10	78.94±0.12	97.14±0.17	95.74±0.05	96.35±0.11	94.83±0.24	87.92±0.18
RadImageNet	91.85±0.04	90.74±0.13	79.89±0.06	76.71±0.10	84.95±0.03	82.45±0.14	87.93±0.22	96.98±0.08	90.18±0.01	75.42±0.06	97.92±0.11	89.01±0.15	91.80±0.21	83.78±0.03	85.94±0.04
UniMed-CLIP	93.27±0.31	91.16±0.06	81.01±0.07	78.38±0.01	84.58±0.14	83.14±0.16	87.94±0.11	97.31±0.16	89.57±0.09	75.99±0.02	97.39±0.12	94.59±0.05	92.77±0.04	94.46±0.30	86.97±0.22
Unimiss+	89.52±0.09	90.26±0.26	76.27±0.03	72.64±0.05	75.86±0.16	83.57±0.03	88.85±0.01	98.49±0.19	91.05±0.15	82.49±0.31	94.57±0.04	84.23±0.17	89.95±0.26	78.30±0.03	83.18±0.05
Ours	95.04±0.13	94.13±0.02	83.20±0.08	79.22±0.01	86.92±0.05	84.66±0.19	89.56±0.15	99.57±0.06	92.80±0.03	86.70±0.79	99.03±0.12	96.50±0.20	97.61±0.04	95.92±0.20	88.24±0.13

Table 6. **Comparison with unified pre-training models.**

		Retinopathy ($\mathcal{D}_1$)									
		APTOS		Glaucoma		IDRiD		PAPILA		Retina	
		ACC↑ (%)	AUC↑ (%)	ACC↑ (%)	AUC↑ (%)	ACC↑ (%)	AUC↑ (%)	ACC↑ (%)	AUC↑ (%)	ACC↑ (%)	AUC↑ (%)
CaSSLe	$\mathcal{D}_0$	90.55±0.07	92.30±0.16	87.14±0.17	90.64±0.02	80.58±0.08	80.17±0.11	85.23±0.20	76.70±0.10	74.90±0.14	73.17±0.01
	$\mathcal{D}_0 \rightarrow \mathcal{D}_1$	91.37±0.02	93.93±0.07	88.69±0.02	92.59±0.14	83.39±0.01	82.31±0.04	86.12±0.14	78.59±0.02	78.68±0.03	86.97±0.11
	$\mathcal{D}_0 \rightarrow \mathcal{D}_1 \rightarrow \mathcal{D}_2$	90.86±0.04	93.14±0.04	88.11±0.07	91.28±0.05	82.67±0.06	81.69±0.01	85.49±0.08	77.67±0.04	77.95±0.15	86.12±0.05
	$\mathcal{D}_0 \rightarrow \mathcal{D}_1 \rightarrow \mathcal{D}_2 \rightarrow \mathcal{D}_3$	90.27±0.10	92.47±0.18	87.84±0.12	91.00±0.01	81.33±0.01	80.14±0.12	85.10±0.01	76.98±0.17	77.36±0.27	85.49±0.24
	$\mathcal{D}_0 \rightarrow \mathcal{D}_1 \rightarrow \mathcal{D}_2 \rightarrow \mathcal{D}_3 \rightarrow \mathcal{D}_4$	89.84±0.03	91.87±0.04	87.20±0.21	90.31±0.03	80.27±0.05	79.58±0.20	84.82±0.17	76.29±0.01	76.94±0.12	85.08±0.10
MedCoss	$\mathcal{D}_0$	90.55±0.07	92.30±0.16	87.14±0.17	90.64±0.02	80.58±0.08	80.17±0.11	85.23±0.20	76.70±0.10	74.90±0.14	73.17±0.01
	$\mathcal{D}_0 \rightarrow \mathcal{D}_1$	91.64±0.11	94.18±0.03	87.91±0.02	92.27±0.06	82.98±0.02	81.57±0.13	86.72±0.31	78.99±0.03	83.57±0.13	86.69±0.20
	$\mathcal{D}_0 \rightarrow \mathcal{D}_1 \rightarrow \mathcal{D}_2$	91.22±0.02	93.87±0.12	87.46±0.04	92.00±0.10	82.34±0.06	81.26±0.22	86.01±0.14	78.15±0.22	83.06±0.02	86.37±0.07
	$\mathcal{D}_0 \rightarrow \mathcal{D}_1 \rightarrow \mathcal{D}_2 \rightarrow \mathcal{D}_3$	90.68±0.04	93.58±0.07	87.22±0.09	91.64±0.08	81.88±0.07	80.37±0.07	85.77±0.07	78.11±0.06	82.55±0.16	86.14±0.11
	$\mathcal{D}_0 \rightarrow \mathcal{D}_1 \rightarrow \mathcal{D}_2 \rightarrow \mathcal{D}_3 \rightarrow \mathcal{D}_4$	90.29±0.06	93.07±0.02	86.47±0.28	91.08±0.13	81.07±0.05	80.16±0.03	85.24±0.12	77.98±0.20	81.69±0.21	85.93±0.04
CoSMIC (ours)	$\mathcal{D}_0$	90.55±0.07	92.30±0.16	87.14±0.17	90.64±0.02	80.58±0.08	80.17±0.11	85.23±0.20	76.70±0.10	74.90±0.14	73.17±0.01
	$\mathcal{D}_0 \rightarrow \mathcal{D}_1$	93.00±0.12	95.39±0.05	89.46±0.25	94.38±0.11	85.84±0.22	83.97±0.23	88.11±0.07	80.10±0.27	87.54±0.06	87.28±0.10
	$\mathcal{D}_0 \rightarrow \mathcal{D}_1 \rightarrow \mathcal{D}_2$	92.85±0.22	95.19±0.02	89.27±0.08	94.27±0.03	85.44±0.01	89.57±0.08	88.06±0.06	79.76±0.04	87.16±0.19	87.12±0.04
	$\mathcal{D}_0 \rightarrow \mathcal{D}_1 \rightarrow \mathcal{D}_2 \rightarrow \mathcal{D}_3$	92.77±0.07	95.13±0.18	89.16±0.01	94.21±0.11	85.27±0.05	83.39±0.05	88.01±0.02	79.46±0.13	86.92±0.09	87.03±0.11
	$\mathcal{D}_0 \rightarrow \mathcal{D}_1 \rightarrow \mathcal{D}_2 \rightarrow \mathcal{D}_3 \rightarrow \mathcal{D}_4$	92.68±0.04	95.04±0.13	89.02±0.07	94.13±0.02	85.17±0.01	83.20±0.08	87.96±0.14	79.22±0.01	86.74±0.08	86.92±0.05

		Radiography($\mathcal{D}_2$)								
		NIH			CXP			SIIM-ARC		
		1%	10%	100%	1%	10%	100%	1%	10%	100%
		AUC↑ (%)	AUC↑ (%)	AUC↑ (%)	AUC↑ (%)	AUC↑ (%)	AUC↑ (%)	Dice↑ (%)	Dice↑ (%)	Dice↑ (%)
CaSSLe	$\mathcal{D}_0$	57.91±0.22	67.51±0.14	80.14±0.03	80.00±0.04	82.08±0.02	86.20±0.04	47.77±0.21	62.69±1.31	72.55±0.04
	$\mathcal{D}_0 \rightarrow \mathcal{D}_1$	55.68±0.13	64.38±0.11	78.72±0.11	78.94±0.03	80.47±0.21	84.58±0.02	44.68±0.65	60.52±0.21	69.85±0.51
	$\mathcal{D}_0 \rightarrow \mathcal{D}_1 \rightarrow \mathcal{D}_2$	61.22±0.04	72.66±0.02	81.34±0.06	80.39±0.20	82.95±0.04	88.88±0.12	47.81±1.12	64.33±1.27	82.33±0.34
	$\mathcal{D}_0 \rightarrow \mathcal{D}_1 \rightarrow \mathcal{D}_2 \rightarrow \mathcal{D}_3$	59.77±0.10	70.94±0.05	80.19±0.07	79.34±0.01	81.36±0.08	88.19±0.17	47.03±0.62	63.11±0.94	80.67±0.69
	$\mathcal{D}_0 \rightarrow \mathcal{D}_1 \rightarrow \mathcal{D}_2 \rightarrow \mathcal{D}_3 \rightarrow \mathcal{D}_4$	58.69±0.08	68.07±0.12	79.38±0.10	78.65±0.12	80.11±0.01	87.86±0.30	45.98±0.99	61.71±1.13	79.77±0.16
MedCoss	$\mathcal{D}_0$	57.91±0.22	67.51±0.14	80.14±0.03	80.00±0.04	82.08±0.02	86.20±0.04	47.77±0.21	62.69±1.31	72.55±0.04
	$\mathcal{D}_0 \rightarrow \mathcal{D}_1$	50.08±0.69	62.58±0.73	75.49±0.09	76.22±0.16	79.89±0.07	82.96±0.09	41.68±1.35	57.63±1.27	62.39±1.58
	$\mathcal{D}_0 \rightarrow \mathcal{D}_1 \rightarrow \mathcal{D}_2$	61.33±0.31	76.98±0.09	82.66±0.13	81.33±0.07	83.85±0.13	88.79±0.01	52.98±1.07	65.88±1.01	84.01±1.22
	$\mathcal{D}_0 \rightarrow \mathcal{D}_1 \rightarrow \mathcal{D}_2 \rightarrow \mathcal{D}_3$	60.67±0.64	74.69±0.11	82.19±0.23	80.64±0.04	83.06±0.14	88.54±0.04	51.73±1.12	64.28±0.54	83.33±0.94
	$\mathcal{D}_0 \rightarrow \mathcal{D}_1 \rightarrow \mathcal{D}_2 \rightarrow \mathcal{D}_3 \rightarrow \mathcal{D}_4$	60.07±0.29	72.88±0.34	81.84±0.02	79.88±0.06	82.31±0.06	88.34±0.03	51.27±0.84	63.89±0.77	82.19±0.30
CoSMIC (ours)	$\mathcal{D}_0$	57.91±0.22	67.51±0.14	80.14±0.03	80.00±0.04	82.08±0.02	86.20±0.04	47.77±0.21	62.69±1.31	72.55±0.04
	$\mathcal{D}_0 \rightarrow \mathcal{D}_1$	57.97±0.19	66.69±0.10	80.26±0.22	79.80±0.05	81.92±0.29	86.12±0.06	46.85±0.45	61.85±0.35	71.49±0.09
	$\mathcal{D}_0 \rightarrow \mathcal{D}_1 \rightarrow \mathcal{D}_2$	69.81±0.09	80.73±0.09	85.11±0.05	83.80±0.04	86.50±0.21	89.78±0.03	55.03±0.58	69.37±1.37	86.90±0.89
	$\mathcal{D}_0 \rightarrow \mathcal{D}_1 \rightarrow \mathcal{D}_2 \rightarrow \mathcal{D}_3$	69.31±0.10	79.40±0.06	84.83±0.11	83.52±0.05	86.46±0.03	89.64±0.02	54.38±0.05	69.07±0.58	86.58±1.06
	$\mathcal{D}_0 \rightarrow \mathcal{D}_1 \rightarrow \mathcal{D}_2 \rightarrow \mathcal{D}_3 \rightarrow \mathcal{D}_4$	69.07±0.22	79.06±0.05	84.66±0.19	83.32±0.12	86.34±0.05	89.56±0.15	53.36±0.26	68.45±0.67	86.70±0.79

		Radiography($\mathcal{D}_2$)											
		ZhangCXR						RSNA					
		1%		10%		100%		1%		10%		100%	
		ACC↑ (%)	AUC↑ (%)	ACC↑ (%)	AUC↑ (%)	ACC↑ (%)	AUC↑ (%)	ACC↑ (%)	AUC↑ (%)	ACC↑ (%)	AUC↑ (%)	ACC↑ (%)	AUC↑ (%)
CaSSLe	$\mathcal{D}_0$	80.74±0.09	87.85±0.04	85.32±0.05	92.87±0.09	93.69±0.10	96.15±0.09	74.94±0.05	82.67±0.07	77.21±0.05	86.54±0.13	82.10±0.12	92.00±0.14
	$\mathcal{D}_0 \rightarrow \mathcal{D}_1$	77.56±0.03	84.36±0.06	83.27±0.07	89.35±0.03	91.39±0.13	94.26±0.03	71.69±0.05	80.33±0.02	74.98±0.07	83.39±0.07	80.64±0.02	89.38±0.09
	$\mathcal{D}_0 \rightarrow \mathcal{D}_1 \rightarrow \mathcal{D}_2$	81.69±0.04	89.08±0.02	86.59±0.04	94.65±0.07	94.56±0.02	98.78±0.01	75.34±0.10	84.56±0.11	76.39±0.01	85.97±0.02	83.67±0.07	91.95±0.10
	$\mathcal{D}_0 \rightarrow \mathcal{D}_1 \rightarrow \mathcal{D}_2 \rightarrow \mathcal{D}_3$	80.08±0.11	88.19±0.05	85.66±0.03	93.25±0.12	93.69±0.19	98.05±0.03	73.98±0.07	83.85±0.02	75.27±0.03	84.69±0.06	82.64±0.04	90.39±0.08
	$\mathcal{D}_0 \rightarrow \mathcal{D}_1 \rightarrow \mathcal{D}_2 \rightarrow \mathcal{D}_3 \rightarrow \mathcal{D}_4$	78.87±0.03	86.39±0.12	84.39±0.01	92.16±0.07	92.22±0.14	97.58±0.12	73.09±0.01	83.00±0.04	74.45±0.03	83.55±0.04	81.96±0.01	89.58±0.22
MedCoss	$\mathcal{D}_0$	80.74±0.09	87.85±0.04	85.32±0.05	92.87±0.09	93.69±0.10	96.15±0.09	74.94±0.05	82.67±0.07	77.21±0.05	86.54±0.13	82.10±0.12	92.00±0.14
	$\mathcal{D}_0 \rightarrow \mathcal{D}_1$	75.69±0.12	83.03±0.06	82.36±0.16	86.67±0.07	87.66±0.07	89.34±0.33	68.77±0.03	77.96±0.08	74.19±0.07	81.11±0.23	77.66±0.31	84.71±0.53
	$\mathcal{D}_0 \rightarrow \mathcal{D}_1 \rightarrow \mathcal{D}_2$	82.33±0.07	87.36±0.02	85.58±0.05	92.33±0.01	94.36±0.07	98.97±0.65	73.55±0.15	83.32±0.13	77.98±0.14	88.39±0.14	81.69±0.27	91.98±0.10
	$\mathcal{D}_0 \rightarrow \mathcal{D}_1 \rightarrow \mathcal{D}_2 \rightarrow \mathcal{D}_3$	81.96±0.18	86.78±0.04	84.79±0.10	91.58±0.04	93.68±0.05	98.39±0.13	72.69±0.01	82.67±0.04	77.18±0.21	87.23±0.23	81.10±0.04	91.22±0.07
	$\mathcal{D}_0 \rightarrow \mathcal{D}_1 \rightarrow \mathcal{D}_2 \rightarrow \mathcal{D}_3 \rightarrow \mathcal{D}_4$	81.11±0.04	86.05±0.07	84.13±0.07	90.26±0.08	92.88±0.04	98.16±0.16	71.89±0.33	81.82±0.11	76.04±0.03	86.76±0.01	80.33±0.13	90.79±0.14
CoSMIC (ours)	$\mathcal{D}_0$	80.74±0.09	87.85±0.04	85.32±0.05	92.87±0.09	93.69±0.10	96.15±0.09	74.94±0.05	82.67±0.07	77.21±0.05	86.54±0.13	82.10±0.12	92.00±0.14
	$\mathcal{D}_0 \rightarrow \mathcal{D}_1$	82.38±0.22	89.68±0.16	86.28±0.13	92.85±0.09	93.56±0.01	96.27±0.24	74.66±0.07	82.62±0.07	77.17±0.10	86.49±0.01	82.00±0.20	91.98±0.16
	$\mathcal{D}_0 \rightarrow \mathcal{D}_1 \rightarrow \mathcal{D}_2$	86.27±0.01	91.58±0.01	91.42±0.11	96.41±0.20	96.54±0.06	99.81±0.15	78.42±0.10	86.41±0.17	79.89±0.03	90.67±0.11	84.33±0.02	93.10±0.21
	$\mathcal{D}_0 \rightarrow \mathcal{D}_1 \rightarrow \mathcal{D}_2 \rightarrow \mathcal{D}_3$	86.22±0.09	91.54±0.15	91.37±0.17	96.39±0.11	96.54±0.04	99.64±0.04	78.40±0.11	86.37±0.09	79.86±0.10	90.64±0.19	84.27±0.25	92.90±0.01
	$\mathcal{D}_0 \rightarrow \mathcal{D}_1 \rightarrow \mathcal{D}_2 \rightarrow \mathcal{D}_3 \rightarrow \mathcal{D}_4$	85.98±0.23	91.27±0.02	91.32±0.25	96.36±0.17	96.27±0.08	99.57±0.06	78.35±0.13	86.32±0.18	79.84±0.08	90.59±0.13	84.19±0.06	92.80±0.03

		Ophthalmology($\mathcal{D}_3$)		Dermoscopy($\mathcal{D}_4$)						
		OCTID		ISIC2016		ISIC2017		ISIC2018		ISIC2018(seg)
		ACC↑ (%)	AUC↑ (%)	ACC↑ (%)	AUC↑ (%)	ACC↑ (%)	AUC↑ (%)	ACC↑ (%)	AUC↑ (%)	Dice↑ (%)
CaSSLe	$\mathcal{D}_0$	91.37±0.07	95.59±0.13	88.65±0.04	91.55±0.21	90.50±0.02	95.20±0.15	91.20±0.15	90.35±0.03	86.48±0.14
	$\mathcal{D}_0 \rightarrow \mathcal{D}_1$	89.98±0.02	94.31±0.08	87.24±0.12	90.33±0.22	89.42±0.31	93.70±0.12	89.71±0.09	88.37±0.04	84.81±0.57
	$\mathcal{D}_0 \rightarrow \mathcal{D}_1 \rightarrow \mathcal{D}_2$	88.76±0.04	93.89±0.15	86.54±0.04	89.14±0.16	88.26±0.17	92.55±0.09	87.32±0.14	86.42±0.15	82.64±0.24
	$\mathcal{D}_0 \rightarrow \mathcal{D}_1 \rightarrow \mathcal{D}_2 \rightarrow \mathcal{D}_3$	93.57±0.07	98.19±0.02	85.73±0.17	88.57±0.26	86.87±0.24	91.18±0.26	86.54±0.15	84.28±0.10	81.42±0.37
	$\mathcal{D}_0 \rightarrow \mathcal{D}_1 \rightarrow \mathcal{D}_2 \rightarrow \mathcal{D}_3 \rightarrow \mathcal{D}_4$	92.39±0.03	97.86±0.14	88.87±0.12	90.20±0.18	90.21±0.05	94.65±0.03	89.38±0.02	87.85±0.03	84.18±0.08
MedCoss	$\mathcal{D}_0$	91.37±0.07	95.59±0.13	88.65±0.04	91.55±0.21	90.50±0.02	95.20±0.15	91.20±0.15	90.35±0.03	86.48±0.14
	$\mathcal{D}_0 \rightarrow \mathcal{D}_1$	86.45±0.14	92.77±0.24	82.44±0.13	86.48±0.34	83.52±0.04	85.99±0.33	84.79±0.24	76.39±0.14	80.25±0.23
	$\mathcal{D}_0 \rightarrow \mathcal{D}_1 \rightarrow \mathcal{D}_2$	85.97±0.06	92.28±0.15	82.36±0.09	86.27±0.17	83.37±0.11	85.67±0.12	84.56±0.18	76.33±0.07	80.39±0.52
	$\mathcal{D}_0 \rightarrow \mathcal{D}_1 \rightarrow \mathcal{D}_2 \rightarrow \mathcal{D}_3$	85.34±0.10	92.64±0.09	82.15±0.17	86.22±0.26	82.99±0.28	85.66±0.34	83.69±0.36	77.21±0.28	80.17±0.26
	$\mathcal{D}_0 \rightarrow \mathcal{D}_1 \rightarrow \mathcal{D}_2 \rightarrow \mathcal{D}_3 \rightarrow \mathcal{D}_4$	93.57±0.07	98.48±0.02	91.22±0.02	92.55±0.13	88.97±0.10	95.31±0.09	88.97±0.20	92.62±0.22	87.52±0.12
CoSMIC (ours)	$\mathcal{D}_0$	91.37±0.07	95.59±0.13	88.65±0.04	91.55±0.21	90.50±0.02	95.20±0.15	91.20±0.15	90.35±0.03	86.48±0.14
	$\mathcal{D}_0 \rightarrow \mathcal{D}_1$	91.24±0.02	95.55±0.13	88.39±0.03	91.06±0.05	90.33±0.15	95.00±0.20	90.74±0.24	90.08±0.10	86.44±0.18
	$\mathcal{D}_0 \rightarrow \mathcal{D}_1 \rightarrow \mathcal{D}_2$	91.21±0.30	95.53±0.03	88.39±0.09	91.19±0.06	90.17±0.06	94.86±0.21	90.67±0.21	90.01±0.03	86.03±0.17
	$\mathcal{D}_0 \rightarrow \mathcal{D}_1 \rightarrow \mathcal{D}_2 \rightarrow \mathcal{D}_3$	96.68±0.18	99.31±0.05	88.13±0.22	90.77±0.13	90.17±0.31	94.86±0.07	90.61±0.21	89.98±0.23	85.79±0.11
	$\mathcal{D}_0 \rightarrow \mathcal{D}_1 \rightarrow \mathcal{D}_2 \rightarrow \mathcal{D}_3 \rightarrow \mathcal{D}_4$	96.28±0.32	99.03±0.12	93.67±0.20	96.50±0.20	94.33±0.22	97.61±0.04	93.45±0.04	95.92±0.20	88.24±0.13

Table 7. **Comparison with continual SSL models in multi-domain medical image analysis**.